Microring Distributed Sensors Using Space-Time Function Control

Montree Bunruangses, Phichai Youplao, Iraj Sadegh Amiri, Nithiroth Pornsuwancharoen, S. Punthawanunt, Ghanshyam Singh, *Senior Member, IEEE*, and Preecha Yupapin

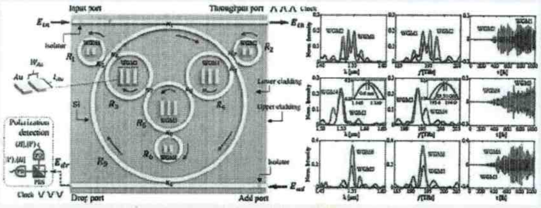

***Abstract*—Distributed microring sensors using space-time function control is proposed for artificial microfacial sensors. The system consists of 6 different node locations, corresponding to the form of the human microfacial structure. Two space-time function input sources are fed into the system simultaneously. The distributed stereo network sensors are investigated. Each sensor node is embedded by a different gold grating period, in which the coupling between the photon and grating generates different plasmonic Bragg wavelengths outputs, which can be used to identify the node positions. The changes introduced to the sensor nodes via the space-time function relationship, such as the polariton (phonon), wavelength, frequency, and temporal change of the Bragg wavelength, can be measured. By using the whispering gallery mode output, the dipole oscillation of each node can be obtained, which can be used for a distributed facial sensor network. The distributed network is connected by the microring coupling in the system. By using the stereo sensor and space-time function sources, a balance of the two-channel sensing signals, known as a stereo sensor, can enable a self-calibration of the sensor, which is achieved. Moreover, exchange between the polariton and electron can be achieved, and electro-optic conversion is obtained. Moreover, the electro-optic conversion obtained by exchanging the polariton and electron energies means that both wireless and cable transmission modes can be employed.**

***Index Terms*—Self-calibration sensors, plasmonic sensors, stereo sensors, distributed sensors, micro-facial sensors.**

I. INTRODUCTION

SILICON oxide has the extraordinary property of enabling the fabrication of microring resonators with a radius up to 1 micron [1]. Therefore, many studies employ silicon microrings [2]–[6]. One microring structure is known as an add-drop multiplexer (filter), which is a promising device that can integrate and function similarly to semiconductor circuits. Both the add-drop multiplexer and microring resonators have a wide range of applications [7]–[11]. A modified add-drop multiplexer called a Panda ring is also useful for various applications [12]–[15], in which additional behaviors are obtained by two side nonlinear phase modulators. Nonlinear rings can couple a nonlinear effect into the main ring, which is useful for the high density and ultrafast switching time of a propagation pulse. In this article, microfacial positions are connected by 6 coupled silicon rings, where the microrings have different radii. Each node is embedded by different gold grating period to produce a polariton dipole oscillation [16], which is a wave-particle behavior. If there is any external coupling to the sensor node, then the coupling between the grating and polariton oscillation introduced by the space-time function sources changes the polariton wave outputs. The plasmonic wave oscillation generated by the excited polariton (phonon) can enable microantenna propagation. In a manipulation, the proposed system is excited by a soliton pulse into a system (micro facial structure) that is modulated by a time function source, where polariton (phonon) transmission forms at each sensor node, which is available for both wireless and

Manuscript received September 18, 2019; accepted October 2, 2019. Date of publication October 7, 2019; date of current version December 31, 2019. This work was supported by Rajamangala University of Technology Phra Nakhon, Bangkok 10200, Thailand. The associate editor coordinating the review of this article and approving it for publication was Dr. Sanket Goel. *(Corresponding author: Preecha Yupapin.)*

M. Bunruangses is with the Department of Computer Engineering, Faculty of Industrial Education, Rajamangala University of Technology Phra Nakhon, Bangkok 10300, Thailand (e-mail: montree.b@rmutp.ac.th).

P. Youplao and N. Pornsuwancharoen are with the Department of Electrical Engineering, Faculty of Industry and Technology, Rajamangala University of Technology Isan, Sakon Nakhon Campus, Sakon Nakhon 47160, Thailand (e-mail: phichai.yo@rmuti.ac.th; nithiroth.po@rmuti.ac.th).

I. S. Amiri and P. Yupapin are with the Computational Optics Research Group, Advanced Institute of Materials Science, Ton Duc Thang University, Ho Chi Minh City 758307, Vietnam, and also with the Faculty of Applied Sciences, Ton Duc Thang University, Ho Chi Minh City 758307, Vietnam (e-mail: irajsadeghamiri@tdtu.edu.vn; preecha.yupapin@tdtu.edu.vn).

S. Punthawanunt is with the Multidisciplinary Research Center, Faculty of Science and Technology, Kasem Bundit University, Bangkok 10250, Thailand (e-mail: suphanchai.pun@kbu.ac.th).

G. Singh is with the Department of Electronics and Communication Engineering (ECE), Malaviya National Institute of Technology Jaipur (MNIT), Jaipur 302017, India (e-mail: gsingh.ece@mnit.ac.in).

Digital Object Identifier 10.1109/JSEN.2019.2945772

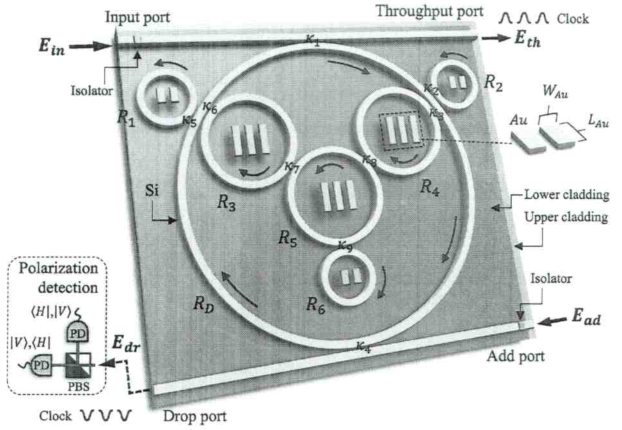

Fig. 1. The proposed microring circuit, where R_1 to R_6, and R_D are the radii of each the ring that fit togetherfor the system. κ_S are the coupling coefficients. E_{in}, E_{th}, E_{dr}, and E_{ad} represent the electrical fields each at the input port, throughput port, drop port, and add port, respectively.

cable systems. A distributed sensor network linked by the time function can transmit to required destinations via the available transmission modes. Node identification is achieved based on the different Bragg wavelength outputs detected at the system ports and the whispering gallery mode (WGM) output, in which the communication among the distributed nodes is distinguished. Information can be encoded by asynchronous multiplexing via the time function (different time multiplexings) transferred to the sensor nodes and network. By using the wave-particle property, both light outputs formed by the whispering gallery mode (WGM) [15], [17], [18] and the throughput port and the particle (polariton and phonon) outputs are detected, which are useful for a photonic transmission. The quantum encoding/decoding process can be achieved by the time function signals processed by the polariton spin orientation, where the quantum codes match the polariton (phonon) cloud codes of each node that is retrieved. More related works of the plasmonic waves are found in the given references for extended reading [19]–[25]. The stereo sensor of the symmetrical system design (i.e. a stereo sensor) is the main point, which can simultaneously realize space-time function control. Simultaneous space-time function control is actually a novel system design, which has never been demonstrated before. A simulation is performed in a graphical program (Optiwave), and MATLAB is applied for verification. The related theoretical background is given. The obtained results show the potential application of a large distributed sensing area, where artificial microrobotic applications are possible. Furthermore, a set of asynchronous multiplexed signals can be coded by the time function carrier, and a stenographic pattern is formed and memorized within the memory cloud.

II. THEORETICAL BACKGROUND

The proposed plasmonic microring stereo sensor system for artificial distributed micro facial sensor is shown in Figure 1. The system consists of 6 different node locations correspond to the form of the human facial structure. Two space-time input sources are fed into the system, and the distributed stereo network sensors are investigated. Each sensor node is embedded by a different gold grating period, which produces different plasmonic Bragg wavelength outputs, and the node location can be identified. The system mechanism and information are described in the following section.

A. The Space Function

The space-function of one dimension given by a soliton pulse in the z-direction as [14], [26]

$$S(z,t) = A\ \mathrm{sech}\left[\frac{T}{T_0}\right]\left[e^{\left(\frac{z}{2L_d}\right)}\right] \tag{1}$$

The phase term and soliton pulse dispersion in the waveguide are neglected because they are included in the simulation via the nonlinear material refractive index calculation. The amplitude of the optical fields is represented by A. The propagation distance is represented by z. The propagation time for a soliton pulse moving with a group velocity in a given frame is $T = t - \beta_1 \times z$. Here, ω_0 is the frequency shift of the soliton. $L_d = T_0^2/|\beta_2|$ represents the dispersion length of the soliton pulse, where T_0 is the soliton pulse propagation time at the initial input. The coefficients of the linear and second-order terms of Taylor's expansion of the propagation constant are β_1 and β_2, respectively. For a soliton pulse in a microring device, a balance should be achieved between the dispersion length (L_d) and the nonlinear length $L_{NL} = 1/\Gamma\phi_{NL}$, where $\Gamma = n_2 K_0$ is the length scale over which the medium is dispersive. For a soliton pulse, there is a balance between dispersion and nonlinear lengths; hence, $L_d = L_{NL}$ [14], [26]. However, in this work, all parameters are obtained from a graphical method, and they are applied and confirmed in a MATLAB program.

B. The Time Function

The photon oscillation in the time given by [28, 29]

$$B \cdot e^{-i\sum_{j=1}^{n}\omega_j t_j} \tag{2}$$

where j = 1 in this case and $\omega_1 t_1 = 2\pi\gamma_1 t_1$. ω_1, γ_1, and t_1 are the angular frequency, linear frequency, and time, respectively. B is a constant. In general, the time function can be a set of signal trains that are applied to a system for processing. When the coding of the time function is not the same, stenographic codes generated [29]. Four-wave mixing within a nonlinear microring resonator is introduced by a nonlinear effect known as the Kerr effect, which is given by the relationship $n = n_0 + n_2 I = n_0 + n_2 P/A_{eff}$, where n_0 and n_2 are the linear and nonlinear refractive indices, respectively. I is the optical intensity, and P is the optical power, where A_{eff} is the effective core mode area of the device. For microring resonators, most effective core mode areas range from 0.1 to 0.50 μm^2 [30].

C. Drude Model

The Drude model of the plasma wave induced by a plasmonic wave on a metal surface depicts the relationship between the plasma wave frequency and electrical power, where in this case the transduction mechanism can be described by the following [9], [16]. At the plasma frequency, the dielectric function changes sign from negative to positive and the real part of the dielectric function becomes zero. The plasma resonance frequency (ω_p) is expressed by

$$\omega_p = \left[\frac{ne^2}{\epsilon_0 m}\right]^{-1/2} \tag{3}$$

The frequency dependent dielectric function of the solid metal is given by

$$\epsilon(\omega) = 1 - \frac{ne^2}{\epsilon_0 m \omega^2} \tag{4}$$

where ϵ_0 is the relative permittivity, n, e, m are the electron density, charge and mass, respectively. ω is the angular frequency. At the resonant frequency (ω_p), called the plasma frequency.

The plasmonic wave oscillation obtained by using an electric field is a longitudinal wave oscillation. By using Maxwell's equations, the TM polarization and exponential decay of the electric field can be obtained. The wavelength of the light source input into the gold grating is λ. The resonance wavelength is related to the Bragg wavelength and given by $\boldsymbol{\lambda_B} = 2\boldsymbol{n_e}\wedge$, where $\boldsymbol{n_e}$ is the effective refractive index of the grating in the waveguide and is the grating period. In this case, the plasma frequency (ω_p) at the Bragg wavelength is obtained by a plot of the Bragg wavelength versus the normalized intensity.

D. Space-Time Function Control and Self-Calibration

The space function is a soliton pulse that is fed into the system to excite the gold grating; consequently, the plasmonic wave and polariton dipoles oscillate at the Bragg wavelength. The reflected transducer information is coupled into the system, which is modulated by the carrier time function and transmitted to the network at the resonant output. The space-time function control is given by

$$\psi(z,t) = \bar{A}\ \mathbf{sech}\left[\frac{T}{T_0}\right]\left[e^{\left[\frac{Z}{2L_d} - i(\varphi_0+\varphi_1)t\right]}\right] = Ae^{-i\left(\varphi_0+\frac{E_n}{n\hbar}\right)t} \tag{5}$$

where $\mathrm{A} = \bar{\mathrm{A}}\ \mathrm{sech}\left[\frac{T}{T_0}\right]\exp\left(\frac{Z}{2L_d}\right)$ and the initial soliton phase is $\varphi_0 = 0$. The soliton phase change generated by the graphical method is $\varphi_1(t)\frac{E_n}{n\hbar} =$, where $\omega_1 = 2\pi\gamma_1 = \frac{E_n}{n\hbar} = \mathrm{nh}\nu$ and $\mathrm{n} = 1, 2, 3\ldots$ It is a synchronous multiplexing scheme. The input sources are simultaneously fed into the system, and the time (t) is the same throughout the paper.

The self-calibration of the sensor system is controlled by the stereo sensor probes, where the left and right channel (probe) signals are perfectly overlapped. The transmission output can be detected at the system ports and the WGM outputs. An optical isolator, filter, and de-multiplexer are also applied. In an application, the transmission is linked with the nerve cells, organs and body for processing, and the transmission is linked by the blood vessels, nerve cells, organs, and body via the blood vessels.

TABLE I
THE SELECTED PARAMETERS OF THE SYSTEM

Parameters	Symbols	Values	Units
Radii of the ring resonator	R_s	1.5 – 10.0	μm
Coupling coefficient	κ	0.5	-
Waveguide loss	α	0.1	dBmm^{-1}
Waveguide core effective area	A_{eff}	0.25	μm^2
Waveguide's refractive index	n_{Si}	3.47	-
Gold grating width	W_{Au}	0.4	μm
Gold grating length	L_{Au}	0.6 – 1.0	μm
Gold grating thickness	-	0.2	μm
Grating period	Λ	0.60-0.75	μm

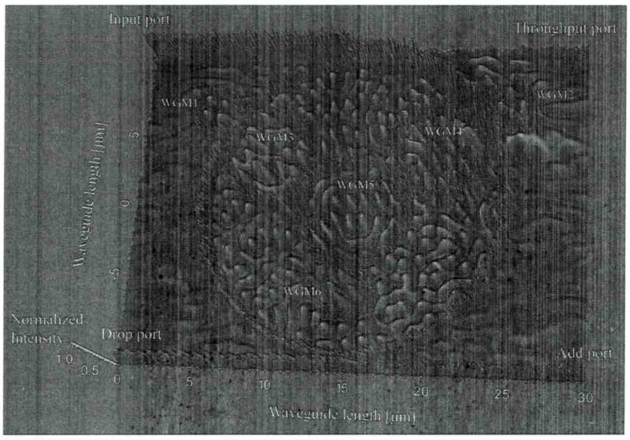

Fig. 2. Graphical results obtained by the Optiwave program. The output is the whispering gallery mode (WGM) at the rings of the circuit, where $R_1 = R_2 = R_6 = 1.5$ μm, and the details of the gold gratings are $W_{Au} = 0.4$ μm and $L_{Au} = 0.6$ μm, with grating periods of 0.60 μm, 0.60 μm, and 0.65 μm, respectively. $R_3 = R_4 = 2.0$ μm, $R_5 = 4.0$ μm, and the details of the gold gratings are $W_{Au} = 0.4$ μm and $L_{Au} = 1.0$ μm, with grating periods of 0.70 μm, 0.70 μm, and 0.75 μm, respectively. All gold gratings are placed 0.5 μm above the lower cladding base. $R_D = 10.0$ μm, $\kappa = 0.5$, and the optical light signals that launch into the system at the input port and the add port have powers of 100 mW, with center wavelength of 1.55 μm and 1.30 μm.

III. SIMULATION RESULTS

The space function is a soliton pulse that is fed into the system to excite the gold grating, and consequently plasmonic wave and polariton dipoles are generated and oscillated at the Bragg wavelength (plasmonic wave). The reflected signals are coupled into the system and transmission line and modulated by the carrier time function before the transmission to the network. By using the resonance condition, suitable parameters are given in Table I and in related figure captions. The graphical result of the system in Figure 1 is shown in Figure 2, and the required suitable parameters are obtained and used for the following figures. The generated WGM output of each sensor node is obtained. In Figure 2, when a system is at the resonant, the pulse intensity fluctuates along the waveguide due to the reflected s light power coupled to the system.

The results obtained from the investigation are shown in Figures 3-6. A plot of the wavelength, frequency, and time signals from the MATLAB program is shown in Figure 3, where (a)-(c) input port from soliton, (d)-(f) throughput

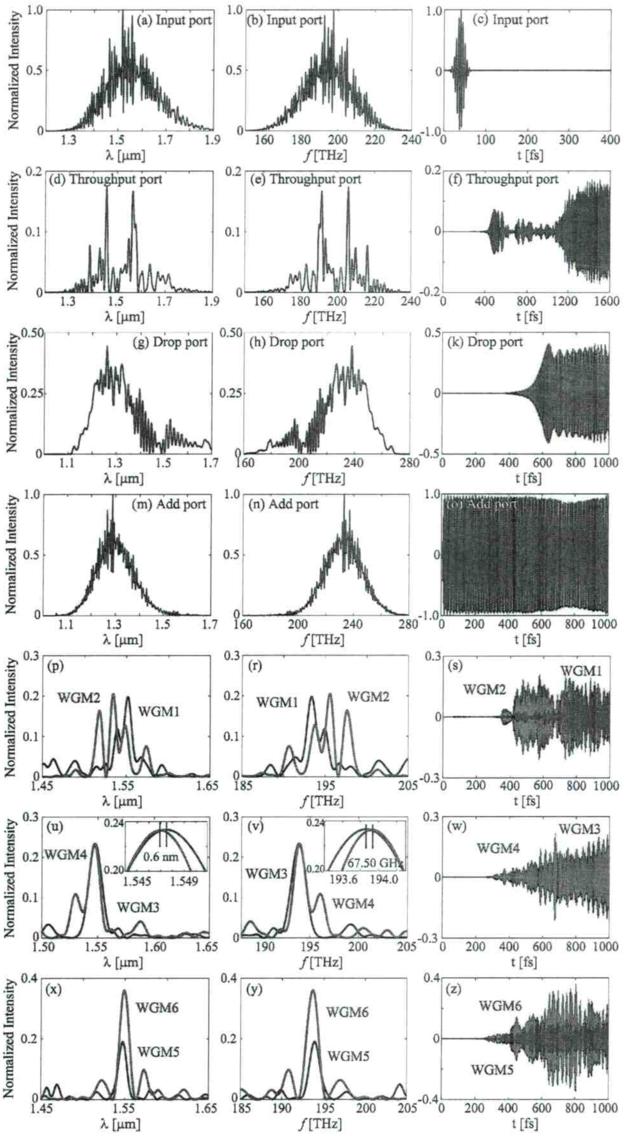

Fig. 3. Simulation results from MATLAB program, where (a)-(c) input port from soliton, (d)-(f) throughput port signals, (g)-(k) drop port signals, (m)-(o) add port signals, (p)-(s) the output signals of WGM1 and WGM2, (u)-(w) the output signals of WGM3 and WGM4, and (x)-(z) the output signals of WGM5 and WGM6.

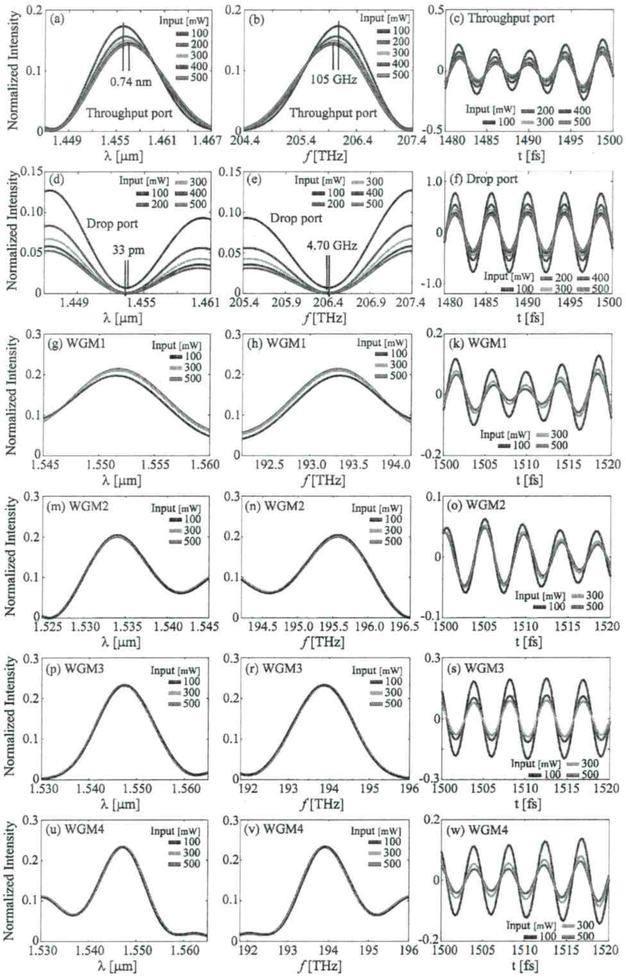

Fig. 4. The results obtained by varying the input powers from 100 mW to 500 mW, where (a)-(c) bright signals from the Throughput port, (d)-(f) dark signals from the Drop port, and (g)-(w) the WGM1, WGM2, WGM3, and WGM4 signals.

port signals, (g)-(k) drop port signals, (m)-(o) add port signals, (p)-(s) the output signals of WGM1 and WGM2, (u)-(w) the output signals of WGM3 and WGM4, and (x)-(z) the output signals of WGM5 and WGM6. The results obtained by varying the input powers from 100 mW to 500 mW are shown in Figure 4, where (a)-(c) and (d)-(f) correspond to the bright signals from the Throughput port and the dark signals from the Drop port, respectively, and (g)-(w) the WGM1, WGM2, WGM3, and WGM4 signals. In Figure 4(c), the oscillation is due to interference between the input signals and the modulated input signals. Figure 5 shows the linearity of the Bragg wavelength shift as a function of the input power, where (a) is the throughput port, (b) is the drop port, (c) is WGM1 and WGM2, and (d) is WGM3 and WGM4. A plot of the MATLAB program results is shown in Figure 6, with the self-calibration stereo sensors of WGM1 and WGM2 and WGM3 and WGM; (a) [WGM-1, WGM-2] and (b) [WGM-3, WGM-4] are obtained with a soliton input power fixed at 100 mW, and the add port power is varied from 100 mW to 500 m; and (c) [WGM-1, WGM-2] and (d) [WGM-3, WGM-4] are obtained with a soliton input power varying from 100 mW to 500 mW, and the add port power is fixed at 100 mW. The use of the obtained results is explained in the following paragraph.

In Figure 3 (a) (the top panel), the pulse in the frequency domain in Throughput port is splitting to two main peaks, which is due to the WGM coupled to the grating generated dipole at the Bragg wavelength. In Figure 4 (a) (the top panel), the bandwidth of the oscillation in throughout port broadened, and the intensity in Throughput port becomes weaker when the input power increased, which affected by the scattering light coupled to the throughput port outputs. In practice, the grating parameter can be adjusted to support the guiding wavelength.

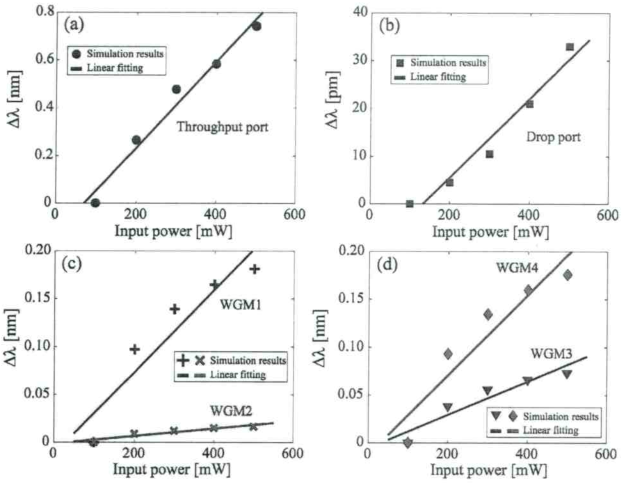

Fig. 5. The linearity trend relation of the wavelength shift as a function of input powers, where (a) throughput port signals, (b) drop port signals, (c) WGM1 and WGM2 signals, and (d) WGM3 and WGM4 signals.

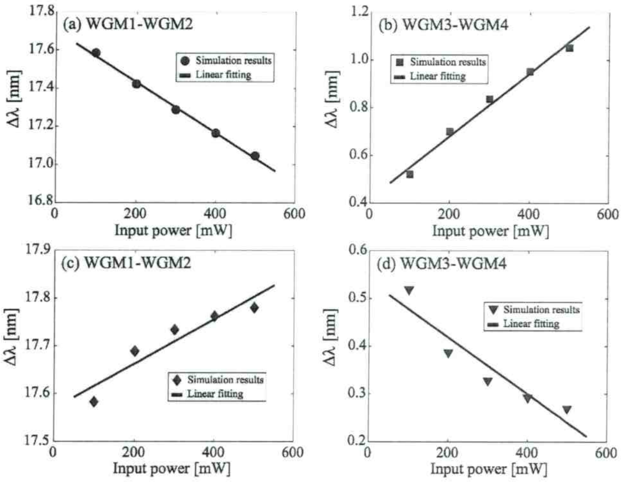

Fig. 6. Results of the MATLAB program, where the self-calibration stereo sensors of WGM1 and WGM2, WGM3 and WGM4, where (a) [WGM-1, WGM-2] and (b) [WGM-3, WGM-4] obtained by soliton input power fixed to 100 mW and add port power is varied from 100 mW to 500 mW, (c) [WGM-1, WGM-2] and (d) [WGM-3, WGM-4] obtained by soliton input power varying from 100 mW to 500 mW and add port power fixed to 100 mW.

Figure 7 shows the plot of the obtained simulation results of the TE mode output with the grating parameters, from which the obtained Bragg wavelength is $2 \times 3.47 \times 0.23 = 1.59$ μm, where the grating period is 0.23 μm. In applications, after the sensor system is resonant, the system is started by confirming the flip-flop pulses from the bright and dark soliton pulses obtained from the through and drop ports [11], [31], respectively. By using synchronous transmission, the change in the polariton cloud of each distributed sensor node induced by the external stimuli is modulated by the time-function signals before the transmission. The set of signals are transferred via the information interaction between the electron cloud and stimuli, from which the quantum bits are generated, sent back into the system cloud (transmission network) and modulated by the incoming carrier (time function), which is now ready for transmission into the cloud network (memory). The resonant recognition pattern retrieved by the comparison process is called a stereo self-calibration, which is the finalized state of the information before the transmission. Quantum consciousness can be processed by time function detection via the polariton polarization (spin) detection arrangement. The induced change in the plasmonic sensor can change the dipole oscillation of each sensor node, which can disturb, shift and change the Bragg wavelength from the initial value. Moreover, the specific gold grating period can be used to identify the Bragg wavelength center. The induced change by the time energy function of each sensor node can disturb and shift the Bragg wavelength from the current value. The specific applied energy can be used to distinguish the energy source. Thus, the change in the space function magnitude can increase the quality of the perception. The change in the energy (frequency) and time can be processed to form a memory by the polariton spins, i.e., quantum codes, where quantum consciousness is formed and localized in the cloud network. If there is one time energy function, then the memory never exists. The combination of space and time functions may have potential for humanoid robotic brain functionalities. A robotic system (brain) driven by a space function can process the command, while the time function can be applied for pattern recognition and memory.

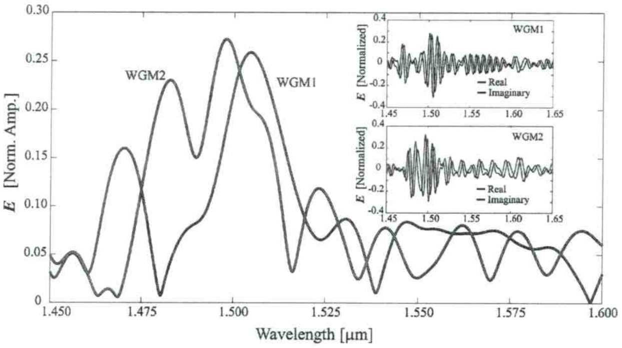

Fig. 7. The output is the whispering gallery mode (WGM) at the ring R_1 and R_2 of the circuit. The details of the gold gratings are $W_{Au} = 0.1$ μm and $L_{Au} = 0.6$ μm, with the same grating periods of 0.23 μm and the optical light signals that launch into the system at the input port and the add port have powers of 100 mW, with center wavelength of 1.55 μm and 1.30 μm, respectively.

IV. CONCLUSIONS

We have proposed a distributed microfacial sensor system using coupled microring resonators for soft material sensing applications. The sensing transducer nodes are microring embedded gold gratings driven by the WGM light beams of a soliton pulse, which are formed by the polariton dipole oscillation at the Bragg wavelengths. The polariton is a quasi-particle generated by plasmonic diploes and oscillates at the plasma (plasmonic wave) frequency. By using the same principle, the induced chance in the plasmonic wave phase (Bragg wavelength), it can be used for futher applications. Simultaneous space-time function control can be applied for a stereo sensor calibration. The induced change in the Bragg wavelength (frequency) of each sensor probe can change the detection output, which can be detected in both cable and wireless connections via the WGM beam with light fidelity (LiFi) and fiber optic cable technology, respectively. Such a system can also be applied as a micro-robotic face and brain and a sensor probe for soft surface sensors. By using the quantum consciousness encoding/decoding format, a micro-distributed network memory may be constructed and used as a micro-robot brain.

ACKNOWLEDGMENTS

The authors would like to acknowledge the research facilities from Ton Duc Thang University, Vietnam.

REFERENCES

[1] A. M. Prabhu, A. Tsay, Z. Han, and V. Van, "Extreme miniaturization of silicon add–drop microring filters for VLSI photonics applications," *IEEE Photon. J.*, vol. 2, no. 3, pp. 436–444, Jun. 2010.

[2] C. Koos, L. Jacome, C. Poulton, J. Leuthold, and W. Freude, "Nonlinear silicon-on-insulator waveguides for all-optical signal processing," *Opt. Express*, vol. 15, no. 10, pp. 5976–5990, 2007.

[3] N. Pornsuwancharoen *et al.*, "Micro-current source generated by a WGM of light within a stacked silicon-graphene-Au waveguide," *IEEE Photon. Technol. Lett.*, vol. 29, no. 21, pp. 1768–1771, Nov. 1, 2017.

[4] H.-M. Xin, Y.-Q. Huang, H.-B. Chen, H. Huang, X. Ren, and X.-G. Zhou, "Design and fabrication of InP micro-ring resonant detectors," *Optoelectron. Lett.*, vol. 5, no. 1, pp. 6–10, 2009.

[5] W. Bogaerts *et al.*, "Silicon microring resonators," *Laser Photon. Rev.*, vol. 6, no. 1, pp. 47–73, 2012.

[6] A. H. Atabaki *et al.*, "Integrating photonics with silicon nanoelectronics for the next generation of systems on a chip," *Nature*, vol. 556, pp. 349–354, Apr. 2018.

[7] P. Youplao *et al.*, "Microring stereon sensors model using Kerr-Vernier effect for Biocel sensor and communication," *Nano Commun. Netw.*, vol. 17, pp. 30–35, 2018.

[8] A. Dutt, K. Luke, S. Manipatruni, A. L. Gaeta, P. Nussenzveig, and M. Lipson, "On-chip optical squeezing," *Phys. Rev. Appl.*, vol. 3, no. 4, 2015, Art. no. 044005.

[9] S. Tunsiri, N. Thammawongsa, T. Threepak, S. Mitatha, and P. Yupapin, "Microring switching control using plasmonic ring resonator circuits for super-channel use," *Plasmonics*, to be published.

[10] J. W. Silverstone *et al.*, "Qubit entanglement between ring-resonator photon-pair sources on a silicon chip," *Nature Commun.*, vol. 6, Aug. 2015, Art. no. 7948.

[11] S. Soysouvanh *et al.*, "Ultra-fast electro-optic switching control using a soliton pulse within a modified add-drop multiplexer," *Microsyst. Technol.*, vol. 24, no. 9, pp. 3777–3782, 2018.

[12] J. Ali *et al.*, "Nano-capacitor-like model using light trapping in plasmonic island embedded microring system," *Results Phys.*, vol. 10, pp. 727–730, Sep. 2018.

[13] K. Chaiwong, K. Tamee, and P. P. Yupapin, "Four-wave mixing (FWM) effects within a micro-optical device," *Int. J. Electron. Elect. Eng.*, vol. 4, no. 3, pp. 1–4, 2016.

[14] T. Phatharaworamet, C. Teeka, R. Jomtarak, S. Mitatha, and P. P. Yupapin, "Random binary code generation using dark-bright soliton conversion control within a PANDA ring resonator," *J. Lightw. Technol.*, vol. 28, no. 19, pp. 2804–2809, Oct. 1, 2010.

[15] N. Sarapat *et al.*, "LiFi up-downlink conversion node model generated by inline successive optical pumping," *Microsyst. Technol.*, vol. 25, no. 3, pp. 945–950, 2019.

[16] A. Derkachova and K. Kolwas, "Size dependence of multipolar plasmon resonance frequencies and damping rates in simple metal spherical nanoparticles," *Eur. Phys. J.-Special Topics*, vol. 144, no. 1, pp. 93–99, 2007.

[17] J. Ali *et al.*, "Coherent light squeezing states within a modified microring system," *Results Phys.*, vol. 9, pp. 211–214, Jun. 2018.

[18] P. Youplao *et al.*, "Plasmonic op-amp circuit model using the inline successive microring pumping technique," *Microsyst. Technol.*, vol. 24, no. 9, pp. 3689–3695, 2018.

[19] J. Yan, X. Liao, S. Ji, and S. Zhang, "MEMS-based thermoelectric–photoelectric integrated power generator," *J. Microelectromech. Syst.*, vol. 28, no. 1, pp. 1–3, 2019.

[20] J. Yan, X. Liao, S. Ji, and S. Zhang, "A novel multi-source micro power generator for harvesting thermal and optical energy," *IEEE Electron Device Lett.*, vol. 40, no. 2, pp. 349–352, Feb. 2018.

[21] A. Farmani, M. Miri, and M. H. Sheikhi, "Analytical modeling of highly tunable giant lateral shift in total reflection of light beams from a graphene containing structure," *Opt. Commun.*, vol. 391, pp. 68–76, May 2017.

[22] A. Farmani, A. Mir, and Z. Sharifpour, "Broadly tunable and bidirectional terahertz graphene plasmonic switch based on enhanced Goos-Hänchen effect," *Appl. Surf. Sci.*, vol. 453, pp. 358–364, Sep. 2018.

[23] A. Farmani, M. Miri, and M. H. Sheikhi, "Design of a high extinction ratio tunable graphene on white graphene polarizer," *IEEE Photon. Technol. Lett.*, vol. 30, no. 2, pp. 153–156, Jan. 15, 2018.

[24] A. Farmani and A. Mir, "Graphene sensor based on surface plasmon resonance for optical scanning," *IEEE Photon. Technol. Lett.*, vol. 31, no. 8, pp. 643–646, Apr. 15, 2019.

[25] A. Farmani, "Three-dimensional FDTD analysis of a nanostructured plasmonic sensor in the near-infrared range," *J. Opt. Soc. Amer. B, Opt. Phys.*, vol. 36, no. 2, pp. 401–407, 2019.

[26] G. P. Agrawal, "Nonlinear fiber optics: Its history and recent progress," *J. Opt. Soc. Amer. B, Opt. Phys.*, vol. 28, no. 12, pp. A1–A10, 2011.

[27] D. H. Wolpert, A. Kolchinsky, and J. A. Owen, "A space–time tradeoff for implementing a function with master equation dynamics," *Nature Commun.*, vol. 10, Apr. 2019, Art. no. 1727.

[28] M. Yessenov, B. Bhaduri, H. E. Kondakci, and A. F. Abouraddy, "Weaving the rainbow: Space-time optical wave packets," *Opt. Photon. News*, vol. 30, no. 5, p. 34, 2019.

[29] X. Zhang, W. Zhang, and S. Wang, "Efficient double-layered steganographic embedding," *Electron. Lett.*, vol. 43, no. 8, pp. 482–483, Apr. 2007.

[30] P. Phatharacorn, S. Chaingga, J. Ali, and P. Yupapin, "Micro-optical probe model using integrated triple microring resonators for vertical depth identification," *Microsyst. Technol.*, vol. 24, no. 8, pp. 3513–3519, 2018.

[31] S. Soysouvanh *et al.*, "Ultrafast all-optical ALU operation using a soliton control within the cascaded *InGaAsP/InP* microring circuits," *Microsyst. Technol.*, vol. 25, no. 2, pp. 431–440, 2019.

Montree Bunruangses received the B.Sc. degree in computer science from Ramkhamhaeng University, Thailand, in 1993, the M.Eng. degree in computer engineering from King Mongkut's Institute of Technology Ladkrabang, Bangkok, Thailand, in 2005, and the D.Eng. degree in computer engineering from Mahanakorn University of Technology, Bangkok, Thailand, in 2011. He is a Lecturer with the Department of Computer Engineering, Faculty of Industry Education, Rajamangala University of Technology Phra Nakhon, Bangkok. He has been performing research on ad hoc networks and security systems.

Phichai Youplao received the B.Eng. degree in electrical engineering from North Eastern University (NEU), Khon Kaen, in 1998, the M.Eng. degree in electrical engineering from Mahanakorn University of Technology (MUT), Bangkok, in 2005, and the D.Eng. degree in electrical engineering from King Mongkut's Institute of Technology Ladkrabang (KMITL), Bangkok, Thailand, in 2013. He is a Lecturer with the Department of Electrical Engineering, Faculty of Industry and Technology, Rajamangala University of Technology Isan, Sakon Nakhon Campus, Sakon Nakhon, Thailand.

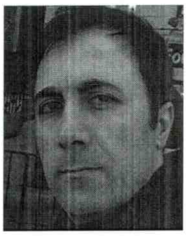

Iraj Sadegh Amiri received the B.Sc. degree in applied physics from the Public University of Oroumiyeh, Iran, in 2001, the M.Sc. (Hons.) degree in physics/optics from University Technology Malaysia (UTM) in 2009, and the Ph.D. degree in physics (photonics) in January 2014. He has been performing research on several topics, such as optical soliton communications, laser physics, plasmonics photonics devices, nonlinear fiber optics, optoelectronics devices using 2D materials, waveguides, quantum cryptography, and nanotechnology engineering.

Nithiroth Pornsuwancharoen received the B.S.Tech.Ed., M.S.Tech.Ed., and Ph.D. in telecommunication engineering and applied physics from King Mongkut's Institute of Technology Ladkrabang (KMITL), Bangkok, Thailand, in 1998, 2005, and 2009, respectively. He is a Lecturer with the Department of Electrical Engineering, Faculty of Industry and Technology, Rajamangala University of Technology Isan, Sakon Nakhon Campus, Sakon Nakhon, Thailand.

S. Punthawanunt received the B.Sc. and M.Sc. degrees in computer science from Assumption University, Bangkok, Thailand. He is currently the Dean of the Faculty of Science, Kasem Bundit University, Bangkok. His research interests are 5G technologies, multimedia communications, and LiFi networking.

Ghanshyam Singh (SM'16) received the B.Tech., M.Tech., and Ph.D. degrees in electronics and communication engineering. He is currently a Professor with the Department of ECE, MNIT Jaipur, India. He had been engaged in joint research with the partner groups from Keio University, Japan, University of Vienna, Austria, LNPU Lviv, Ukraine, and Cairo University, Egypt. He is working on a Joint Research Project with the Group from Kasetsart University, Bangkok, Thailand. His current research interest includes micro/ nanostructured photonic devices, all-optical circuits and networks, the nonlinear characteristics of photonic crystal fibers, integrated photonics, and photonic sensors. He is a Senior Member of the SPIE and OSA and a Fellow of the OSI and IETE. He was a recipient of the Distinguished Lecturer Award from the IEEE Photonics Society for the term 2017 to 2018.

Preecha Yupapin received the Ph.D. degree in electrical engineering from Imperial College and the City, University of London, U.K., in 1993. He is currently a Full Research Professor with the Advanced Institute of Materials Science (AIMaS), Ton Duc Thang University, Ho Chi Minh City, Vietnam. His current research interests are plasmonic electronics, microring resonators, computational optics, quantum optics and engineering, brain science, and quantum consciousness. He is a member of the Thai Institute Physics (TIP), the South East Asia Theoretical Physics Association (SEATPA) committee, and the Optical Society of America (OSA). He has become a hyperprolific author recognized by *Nature* since 2018. He has been a member of the Asian Council of Science Editors Cabinet since 2019.

3956 IEEE SENSORS JOURNAL, VOL. 20, NO. 7, APRIL 1, 2020 IEEE Sensors Council

Comments and Corrections

Correction to “Microring Distributed Sensors Using Space-Time Function Control”

Montree Bunruangses, Phichai Youplao, Iraj Sadegh Amiri, Nithiroth Pornsuwancharoen, S. Punthawanunt, Ghanshyam Singh, *Senior Member, IEEE*, and Preecha Yupapin

Unfortunately, we had mistaken some necessary sentences within the first paragraph in the footnote section and the acknowledgment section of the above article [1], which are required from the first author's affiliation so that the research project can attain the research grant support. The correct sentences within the two sections are given here.

ACKNOWLEDGMENTS

The authors would like to acknowledge the research facilities from Rajamangala University of Technology Phra Nakhon, Bangkok, Thailand, and Ton Duc Thang University, Vietnam.

REFERENCES

[1] M. Bunruangses *et al.*, “Microring distributed sensors using space-time function control,” *IEEE Sensors J.*, vol. 20, no. 2, pp. 799–805, Jan. 2020.

Manuscript received February 3, 2020; accepted February 3, 2020. Date of current version March 5, 2020. This work was supported by the Rajamangala University of Technology Phra Nakhon, Bangkok, Thailand. *(Corresponding author: Preecha Yupapin.)*

Montree Bunruangses is with the Department of Computer Engineering, Faculty of Industrial Education, Rajamangala University of Technology Phra Nakhon, Bangkok 10300, Thailand (e-mail: montree.b@rmutp.ac.th).

Phichai Youplao and Nithiroth Pornsuwancharoen are with the Department of Electrical Engineering, Faculty of Industry and Technology, Rajamangala University of Technology Isan, Sakon Nakhon Campus, Sakon Nakhon 47160, Thailand (e-mail: phichai.yo@rmuti.ac.th; nithiroth.po@rmuti.ac.th).

Iraj Sadegh Amiri and Preecha Yupapin are with the Computational Optics Research Group, Advanced Institute of Materials Science, Ton Duc Thang University, Ho Chi Minh City 758307, Vietnam, and also with the Faculty of Applied Sciences, Ton Duc Thang University, Ho Chi Minh City 758307, Vietnam (e-mail: irajsadeghamiri@tdtu.edu.vn; preecha.yupapin@tdtu.edu.vn).

S. Punthawanunt is with the Multidisciplinary Research Center, Faculty of Science and Technology, Kasem Bundit University, Bangkok 10250, Thailand (e-mail: suphanchai.pun@kbu.ac.th).

Ghanshyam Singh is with the Department of Electronics and Communication Engineering (ECE), Malaviya National Institute of Technology Jaipur (MNIT), Jaipur 302017, India (e-mail: gsingh.ece@mnit.ac.in).

Digital Object Identifier 10.1109/JSEN.2020.2971799

เอกสารแสดงค่า Impact factor ของวารสารตามฐานข้อมูล Web of Science ที่มีค่า Impact factor อ้างอิงตามฐานข้อมูล JCR (Journal Citation Reports)

IEEE SENSORS JOURNAL

ISSN / eISSN **1530-437X / 1558-1748**
Publisher **IEEE-INST ELECTRICAL ELECTRONICS ENGINEERS INC, 445 HOES LANE, PISCATAWAY, USA, NJ, 08855-4141**

General Information

Journal Website	Visit Site	**Publisher Website**	Visit Site
1st Year Published	2001	**Frequency**	Semi-monthly
Issues Per Year	24	**Country**	UNITED STATES OF AMERICA
Primary Language	English	**Submission Website**	Visit Site

Web of Science Coverage

***Web of Science* Core Collection**
Science Citation Index Expanded

Additional *Web of Science* Indexes
Current Contents Engineering, Computing & Technology
Essential Science Indicators

Categories: Engineering, Electrical & Electronic | Physics, Applied | Instruments & Instrumentation | Engineering | Instrumentation & Measurement

Log into *Web of Science* to discover research literature from this journal.

Journal Metrics

2018 Journal Impact Factor 3.076

Categories: Engineering, Electrical & Electronic | Physics, Applied | Instruments & Instrumentation

For the full context of the Journal Impact Factor, access *Journal Citation Reports* to view detailed metrics for this journal.

Peer Review Information

Transparent Peer Review Participant	No	**Sign Report**	No
Publish Report	No	**Publons Reviews**	3,779
Publons Endorsements	65	**Publons Partner**	Yes

Register for a free *Publons* account for more peer review information about this journal.

Editorial Disclaimer: As an independent organization, Clarivate Analytics does not become involved in and is not responsible for the editorial management of any journal or the business practices of any publisher. Publishers are accountable for their journal performance and compliance with ethical publishing standards. The views and opinions expressed in any journal are those of the author(s) and do not necessarily reflect the views or opinions of Clarivate Analytics.

Criteria for selection of newly submitted titles and re-evaluation of existing titles in the Web of Science are determined by the Web of Science Editors in their sole discretion. If a publisher's editorial policy or business practices negatively impact the quality of a journal, or its role in the surrounding literature of the subject, the Web of Science Editors may decline to include the journal in any Clarivate Analytics' product or service. The Web of Science Editors, in their sole discretion, may remove titles from coverage at any point if the titles fail to maintain our standard of quality, do not comply with ethical standards, or otherwise do not meet the criteria determined by the Web of Science Editors. If a journal is deselected or removed from coverage, the journal will cease to be indexed in the Web of Science from a date determined by the Web of Science Editors in their sole discretion – articles published after that date will not be indexed. The Web of Science Editors' decision on all matters relating to journal coverage will be final.

Our policy towards the use of cookies

All Clarivate Analytics websites use cookies to improve your online experience. They were placed on your computer when you launched this website. You can change your cookie settings through your browser.

IEEE Sensors Journal

The IEEE Sensors Journal is a peer-reviewed, semi-monthly online journal devoted to sensors and sensing phenomena. The first issue of IEEE Sensors Journal published in the year 2001 after the motion for its approval was passed at the February 2000 TAB meeting.

3.076
Impact Factor

0.023290
Eigenfactor

0.554
Article Influence Score

Rapid Publication

Submission-to-ePublication = 6.8 weeks, median

Peer Review – The articles in this journal are peer reviewed in accordance with the requirements set forth in the IEEE Publication Services and Products Board Operations Manual. Each published article was reviewed by a minimum of two independent reviewers using a single-blind peer review process, where the identities of the reviewers are not known to the authors, but the reviewers know the identities of the authors. Articles will be screened for plagiarism before acceptance.

The fields of interest of the IEEE Sensors Journal are the theory, design , fabrication, manufacturing and applications of devices for sensing and transducing physical, chemical and biological phenomena, with emphasis on the electronics and physics aspect of sensors and integrated sensors-actuators. IEEE Sensors Journal deals with the following:

- Sensor Phenomenology, Modelling, and Evaluation
- Sensor Materials, Processing, and Fabrication
- Chemical and Gas Sensors

- Microfluidics and Biosensors
- Optical Sensors
- Physical Sensors: Temperature, Mechanical, Magnetic, and others
- Acoustic and Ultrasonic Sensors
- Sensor Packaging
- Sensor Networks
- Sensor Applications
- Sensor Systems: Signals, Processing, and Interfaces
- Actuators and Sensor Power Systems
- Sensor Signal Processing for high precision and stability (amplification, filtering, linearization, modulation/demodulation) and under harsh conditions (EMC, radiation, humidity, temperature); energy consumption/harvesting
- Sensor Data Processing (soft computing with sensor data, e.g., pattern recognition, machine learning, evolutionary computation; sensor data fusion, processing of wave e.g., electromagnetic and acoustic; and non-wave, e.g., chemical, gravity, particle, thermal, radiative and non-radiative sensor data, detection, estimation and classification based on sensor data)
- Sensors in Industrial Practice

Growth of Sensors Journal may be found here.

Editorial Board

Current Issue, Past Issues and Early Access (preprints).

50 Most Accessed Articles – updated monthly, on about the 15th

Special issues published and in preparation

List of all review papers – since 2001

For Authors

Manuscript Submission Portal

ORCID is now compulsory!

Guide for Authors

Keywords for Manuscript Classification

IEEE Copyright Form

- **For Authors**
- Guide for Expanding Conference Papers
- Guidelines for Comments and Reply
- Author Ethics Guidelines

- **For Reviewers**
- Guide for Reviewers

- **For Associate Editors**
- Associate Editor Manual
- Associate Editor Reference Guide
- Nomination and Appointment Form
- Expertise Grid Form
- Special Issues Proposal Form

PUBLICATIONS

- IEEE Sensors Letters
- IEEE Sensors Journal
- IEEE Internet of Things Journal
- IEEE J-ERM
- IEEE T-Big Data
- IEEE T-CAIG
- Top Search Terms & Most Downloaded
- Membership and Subscription Catalog
- Digital Library Subscriptions
- Set Content Alerts

CONFERENCES

- IEEE SENSORS
- IEEE Inertial Sensors
- IEEE VCACS
- Other Cosponsored Conferences
- IEEE ISOEN
- IEEE WF IoT

Education

- Distinguished Lecturers
- Tutorials
- Review Papers
- Awards & Fellows

Home Accessibility IEEE Privacy Policy Non Discrimination Policy

A not-for-profit organization, IEEE is the world's largest technical professional organization dedicated to advancing technology for the benefit of humanity.

Privacy - Terms